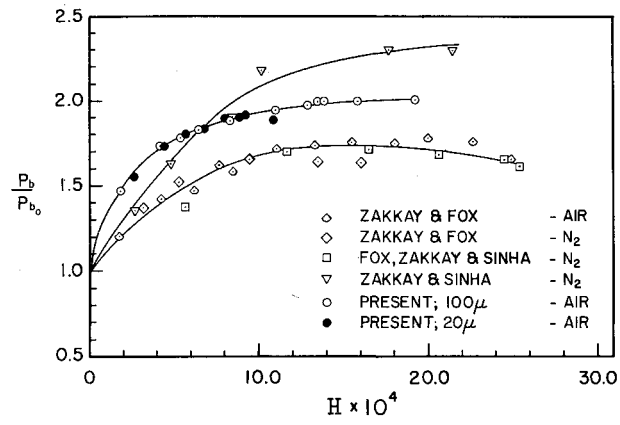

Fig. 3 Porous base injection at Mach 4.0.

injection duct has a very significant influence on the variation of base pressure with mass injection flow rate, because the second maximum is only found for the subsonic nozzle injection case. This second maximum should not be confused with the increase of base pressure at very large mass injection rates as described by Reid and Hastings.[3] Another possible indication of the injection duct influence is that, although the zero mass injection base pressures are decreasing with increasing free stream Mach number in accordance with Ref. 9, the maximum base pressure with mass injection does not follow this trend consistently.

Based on the above results, it is apparent that the most effective injection technique is to introduce the secondary fluid through a porous plate which covers the whole base of the axisymmetric body. The present results for this configuration are compared with other available data in Fig. 3. For all four experiments, the nominal free stream Mach number was 4.0, and the approaching boundary layer was turbulent. However, the reference base pressure ratios varied significantly. Specifically, Zakkay and Fox,[5] Fox, Zakkay, and Sinha,[6] and Zakkay and Sinha,[7] using the same wind tunnel and essentially the same test conditions, reported values of the base pressure at zero mass injection of 0.413, 0.435, and 0.357, respectively. According to Sinha,[10] the results of Refs. 5 and 6 may have been affected by possible nonuniformities in the approaching freestream and misalignment of the streamlined centerbody.

The present data show that the base pressure can be increased by 100% of its sealed base value with mass injection. For an actual vehicle, this would provide for a substantial decrease of the base drag contribution to the total drag. However, before these data can be considered for design calculations, the previously mentioned discrepancies in the reference base pressure values must be resolved.

The present data, as well as that in Refs. 4–6 and 7, show an initial monotonic increase of base pressure with increasing mass flow. However, contrary to the speculation of Bowman and Clayden,[4] the base pressure reaches a plateau value, and then decreases with further increases in the mass injection rate. Measurements at very large mass flow rates were reported by Zakkay and Sinha.[7] As can be seen from Fig. 3, the influence of injection plate porosity on the base pressure is negligible.

References

[1] Cortright, E. M., Jr. and Schroeder, A. H., "Preliminary Investigation of Effectiveness of Base Bleed In Reducing Drag of Blunt-Base Bodies In Supersonic Stream," RME51A26, March 1951, NACA.

[2] Korst, H. H., Page, R. H., and Childs, M. E., "A Theory For Base Pressures in Transonic and Supersonic Flow," ME-TN-392-2, March 1955, University of Illinois, Urbana, Ill.

[3] Reid, J. and Hastings, R. C., "The Effect of a Central Jet on the Base Pressure of a Cylindrical After-Body In a Supersonic Stream," R & M 3224, Dec. 1959, Aeronautical Research Council.

[4] Bowman, J. E. and Clayden, W. A., "Cylindrical Afterbodies in Supersonic Flow With Gas Ejection," *AIAA Journal*, Vol. 5, No. 8, Aug. 1967, pp. 1524–1525.

[5] Zakkay, V. and Fox, H., "Experimental and Analytical Consideration of Turbulent Heterogeneous Mixing In the Wake," NYU-AA-66-54, April 1965, New York University, New York.

[6] Fox, H., Zakkay, V., and Sinha, R., "A Review of Problems in the Nonreacting Turbulent Far Wake," *Astronautica Acta*, Vol. 14, No. 3, 1969, pp. 215–228.

[7] Zakkay, V. and Sinha, R., "An Experimental Investigation of the Near Wake in an Axisymmetric Supersonic Flow with and without Base Injection," *Israel Journal of Technology*, Vol. 7, No. 1–2, 1969, pp. 43–53.

[8] Sieling, W. R., Przirembel, C. E. G., and Page, R. H., "Axisymmetric Turbulent Near Wake Studies at Mach Four: Blunt and Hemispherical Bases," RU-TR 122-MAE-F, OSR 68-2465, Nov. 1968, Rutgers University, New Brunswick, N.J.

[9] Przirembel, C. E. G. and Page, R. H., "Analysis of Axisymmetric Supersonic Turbulent Base Flow," *Proceedings of the 1968 Heat Transfer and Fluid Mechanics Institute*, edited by A. F. Emery and C. A. Depew, Stanford University Press, 1968, pp. 258–272.

[10] R. Sinha, personal communication, June 1970, Singer-General Precision, Inc., Little Falls, N. J.

Time-Dependent Solutions of Nonequilibrium Nozzle Flows—A Sequel

JOHN D. ANDERSON JR.†
U. S. Naval Ordnance Laboratory, White Oak, Silver Spring, Md.

THE solution of steady-state, nonequilibrium, quasi-one-dimensional nozzle flows by means of a numerical, time-dependent technique is described in Ref. 1. This analysis employed a Taylor's series to obtain the flowfield variables in steps of time, starting with assumed initial distributions throughout the nozzle

$$g(x,t + \Delta t) = g(x,t) + (\partial g/\partial t)_t \Delta t + (\partial^2 g/\partial t^2)_t \Delta t^2/2 \quad (1)$$

where g can be any dependent variable such as ρ, T, u, etc., and where the time derivatives are evaluated at time t. The steady-state solution, which is the desired result, is approached at large times. The advantages of this approach, as well as the details of the analysis, are described in Ref. 1; hence, no further elaboration will be given here. However, emphasis is made that Eq. (1), containing three terms of the Taylor's series, is of the second-order accuracy, and that the second-order term is absolutely necessary for stability.

This Note, which is a sequel to Ref. 1, describes the application of a new time-dependent, finite-difference scheme which employs only the first two terms of a series expansion in time,

$$g(x,t + \Delta t) = g(x,t) + (\partial g/\partial t)_{\text{ave}} \Delta t \quad (2)$$

Here, the time derivative is not evaluated at time t as previously; rather, an average value between t and $(t + \Delta t)$ is utilized. This average value is obtained from the general method of MacCormack,[2] who has shown that the general scheme is of second-order accuracy.‡ This new scheme, ap-

Received July 13, 1970; revision received September 14, 1970. This work was supported by the NOL Independent Research funds.

† Chief, Hypersonics Group, Aerophysics Division. Member AIAA.

‡ Acknowledgment is gratefully made to G. Moretti, Polytechnic Institute of Brooklyn, who brought MacCormack's scheme to the author's attention.

plied to nonequilibrium nozzle flows in the present Note, gives results identical to those obtained in Ref. 1, but with fewer computations, hence leading to a reduction in computer time of at least 30%. Since calculations of complex nonequilibrium nozzle flows can be lengthy for certain cases, this reduction can represent a substantial savings. Moreover, the already straightforward and simple analysis of nonequilibrium nozzle flows described in Ref. 1 is made even simpler by the present scheme. The numerical details of this scheme are described in Ref. 3; hence, for brevity, they will not be discussed here.

To illustrate the preceding comments, consider the rapid, nonequilibrium expansion of a vibrationally excited mixture CO_2-N_2-H_2O through a convergent-divergent nozzle, wherein the detailed vibrational energy exchange mechanisms result in a population inversion between the (001) and (100) vibrational levels in CO_2. This example is chosen because of its current interest for gas dynamic lasers; however, the intent of the present Note is to examine and compare the numerical behavior of Eq. (1), hereinafter designated the "three-term method," and Eq. (2), hereafter designated the "two-term method." The physical aspects of this expansion process, as well as details of its analysis, will not be discussed here; they can be found in Refs. 4 and 5 [which use Eq. (1)] and in Ref. 3 [which uses Eq. (2)]. Figure 1 gives the steady-state distributions of the vibrational temperatures for the upper (001) and lower (100) laser levels in CO_2, as well as the translational temperature. Agreement between the two methods is excellent. Similar agreement between the two methods is also obtained for the steady-state population inversion distributions through the nozzle.[3]

Figure 1 illustrates that, for practical purposes, the two methods yield identical steady-state solutions. However, the transient variation during the approach to the steady state can occasionally be quite different between Eqs. (1) and (2). Consider a fixed location in the supersonic section of the nozzle. For the same nozzle expansion, Fig. 2 illustrates the temporal behavior of $\partial(\rho/\rho_0)/\partial t'$ at this location as the time-dependent solution begins from the arbitrary initial conditions and proceeds towards the steady state. Here the time derivatives predicted by the two methods follow similar paths; in both methods, the derivatives become very small as

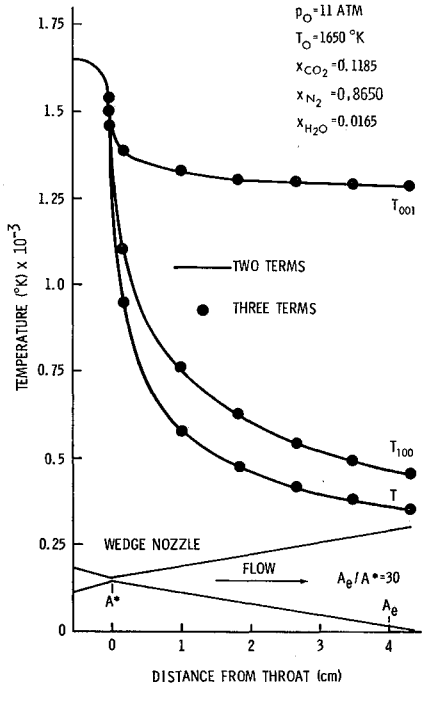

Fig. 1 Steady-state vibrational and translational temperature distributions through a wedge nozzle; comparison of the two methods.

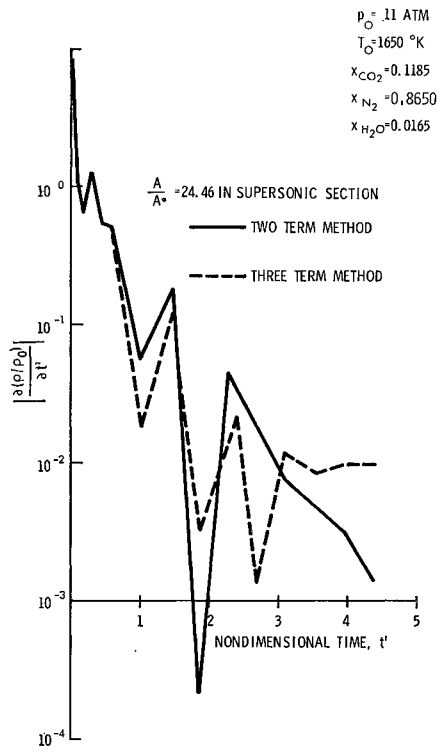

Fig. 2 Transient variation of the density time derivative at a fixed location in the supersonic section.

time progresses. The final steady-state value for ρ/ρ_0 differs by only 0.93% between the two methods. On the other hand, Fig. 3 illustrates the temporal variation of $\partial(\rho/\rho_0)/\partial t'$ at a fixed location in the subsonic section. Here, a striking difference is observed between the two methods. The three-term method yields a derivative which is plateauing whereas the two-term method gives a result which is plunging towards zero as time progresses—a much more satisfying behavior. Despite the differences shown in Fig. 3, the two methods yield steady-state values for ρ/ρ_0 which differ by only 0.12%. Additional comparisons are discussed in Ref. 3.

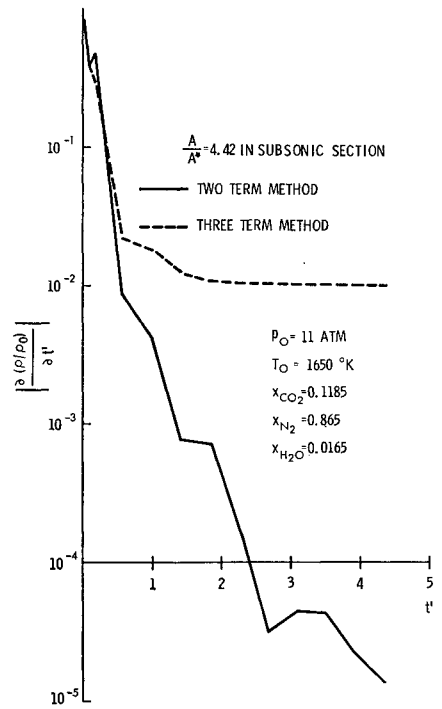

Fig. 3 Transient variation of the density time derivative at a fixed location in the subsonic section.

The behavior of the three-term method shown in Fig. 3 is explained as follows. Returning to Eq. (1), there is the numerical possibility that a steady state can be achieved where $(\partial g/\partial t)_t$ and $(\partial^2 g/\partial t^2)_t$ do not approach zero, but rather the first-and second-order terms in Eq. (1) eventually become of equal magnitude and opposite in sign, hence cancelling and resulting in a stationary value for g from one time step to the next. In previous applications of the time-dependent method employing Eq. (1),[1,4,5,6,7] this behavior was not observed; in all cases, both time derivatives in Eq. (1) became very small as the steady state was approached. However, occasionally the aforementioned anomalous behavior can occur in practice, and such a case is illustrated in Fig. 3. Such remote anomalies do not occur with the present two-term method.

In conclusion, the two-term and three-term methods yield essentially identical steady-state results for nonequilibrium nozzle flows. However, the two-term method [Eq. (2)] discussed in the present Note must be considered superior because it requires less algebra, it requires fewer computations, hence less computer time, and the time derivatives rapidly approach zero in all situations. Hence, the already straightforward and simple analysis of nonequilibrium nozzle flows described in Ref. 1 is made even simpler by the present modification.

References

[1] Anderson, J. D., Jr., "A Time-Dependent Analysis for Vibrational and Chemical Nonequilibrium Nozzle Flows," *AIAA Journal*, Vol. 8, No. 3, March 1970, pp. 545–550.

[2] MacCormack, R. W., "The Effect of Viscosity in Hypervelocity Impact Cratering," AIAA Paper 69-354, Cincinnati, Ohio, 1969.

[3] Anderson, J. D., Jr., "Numerical Experiments Associated with Gas Dynamic Lasers," NOLTR 70-198, Sept. 1970.

[4] Anderson, J. D., Jr., "Time-Dependent Analysis of Population Inversions in an Expanding Gas," *The Physics of Fluids*, Vol. 13, No. 8, Aug. 1970, pp. 1983–1989.

[5] Anderson, J. D., Jr., "A Time-Dependent Quasi-One-Dimensional Analysis of Population Inversions in an Expanding Gas," NOLTR 69-200, Dec. 1969, U. S. Naval Ordnance Lab., White Oak, Md.

[6] Anderson, J. D., Jr., Albacete, L. M., and Winkelmann, A. E., "On Hypersonic Blunt Body Flow Fields Obtained with a Time-Dependent Technique," NOLTR 68-129, Aug. 1968, U. S. Naval Ordance Lab., White Oak, Md.

[7] Anderson, J. D., Jr., "A Time-Dependent Analysis for Quasi-One-Dimensional Nozzle Flows with Vibrational and Chemical Nonequilibrium," NOLTR 69-52, May 1969, U. S. Naval Ordnance Lab., White Oak, Md.

A Direction-Indicating Color Schlieren System

GARY S. SETTLES*

University of Tennessee, Knoxville, Tenn.

THE conventional black-and-white Toepler schlieren system[1,2] displays only those refractive index gradients which deflect light normal to its knife-edge. Other monochrome schlieren methods have been developed to overcome this disadvantage,[3,4] but these methods have limited utility as a result of difficulties with loss of information on gradient directions, separate images, and the compromise between sensitivity and image resolution.

Received August 19, 1970.

* Undergraduate Student, Mechanical and Aerospace Engineering Department. Student Member AIAA.

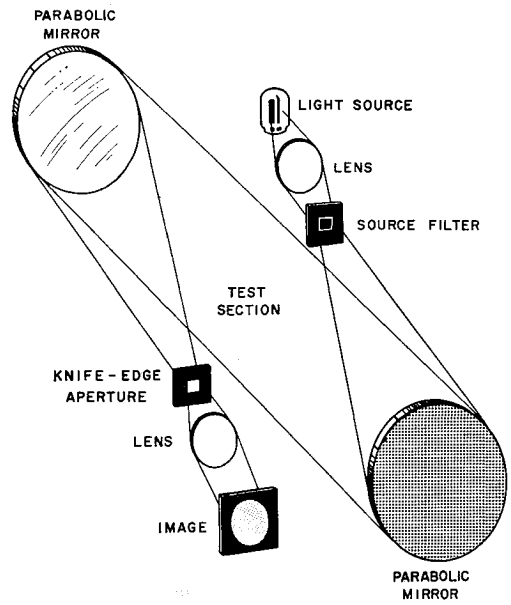

Fig. 1 Arrangement of direction-indicating color schlieren system.

The new color schlieren system described in this Note produces a single image, in which refractive index gradients n all radial directions are displayed and directionally color-coded. In addition, this schlieren system has sensitivity and resolution capabilities comparable to those of the single knife-edge monochrome schlieren, and uses essentially the same optical components as the monochrome schlieren.

A diagram of the new color schlieren system is shown in Fig. 1. The system consists of a white light source, a lens, a color source filter arrangement, two parabolic mirrors, a knife-edge aperture, and a camera lens and screen. These components are arranged in the standard Z-type schlieren configuration.

The source filter, which is illustrated in Fig. 2, breaks the schlieren light beam up into four color bands, which are arranged in a square. The beam proceeds from the source filter to the first parabolic mirror, where it is collimated. The collimated beam passes through the test section and is refocussed by the second parabolic mirror to form an image of the color source bands at the knife-edge location. A square knife-edge aperture cuts off about half of the light of each color, but allows the remaining light to form a schlieren image on the screen.

In going from the source filter to the first parabolic mirror, light of the four colors overlaps and mixes to form a beam of

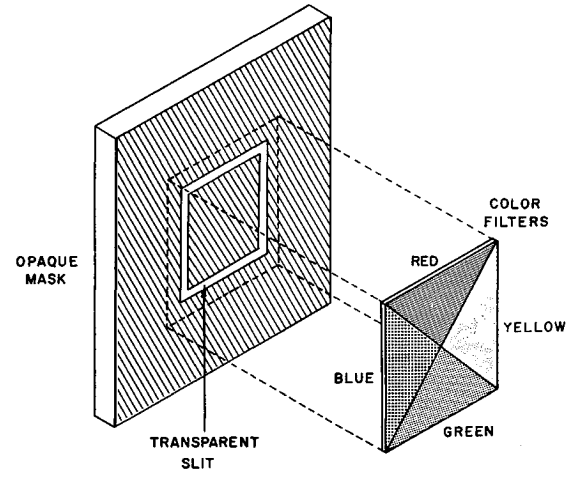

Fig. 2 Source filter assembly.